

## 基于声光效应的谐波锁模光纤激光器中的复杂多脉冲相互作用现象

张欣桐<sup>1,2</sup>, 汪晓聪<sup>1,2</sup>, 黄绮<sup>3</sup>, 黄志远<sup>2</sup>, 罗卓昭<sup>5</sup>, 周耕稷<sup>2</sup>,  
江昕<sup>4,5</sup>, 冷雨欣<sup>2,3\*\*</sup>, 庞盟<sup>1,2,3\*</sup>

<sup>1</sup>中国科学技术大学光学与光学工程系, 安徽 合肥 230026;

<sup>2</sup>中国科学院上海光学精密机械研究所强场激光物理国家重点实验室, 上海 201800;

<sup>3</sup>中国科学院大学杭州高等研究院物理与光电工程学院, 浙江 杭州 310013;

<sup>4</sup>马克斯普朗克光科学研究所罗素学部, 德国 埃朗根 91058;

<sup>5</sup>武汉理工大学光纤传感技术国家工程实验室, 湖北 武汉 430070

**摘要** 脉冲光孤子相互作用的动力学行为在超快脉冲激光和光孤子通讯等领域有着重要的研究价值和前景。锁模光纤激光器作为产生、观测及操控超快孤子脉冲的优秀非线性平台, 推动了孤子动力学领域的快速发展。利用基于光子晶体光纤中高频声光效应的被动锁模光纤激光器, 研究了大量光孤子的复杂相互作用。光纤激光器腔内的高频声光相互作用产生的相对稳定的光机晶格将激光器分割成了数百个相互独立的势阱, 每个势阱可束缚非稳态的多个光孤子, 形成了一种宏观(光机晶格)稳定, 局部(每个势阱内)存在剧烈脉冲间相互作用的亚稳态工作状态。在实验中, 对激光器的偏振态进行调节可实现势阱中孤子数量和孤子能量的调控。研究结果表明, 基于光子晶体光纤中声光效应的高频脉冲激光器可被用来研究大量光孤子脉冲的复杂相互作用, 有望为孤子动力学的研究提供新的思路和有潜力的研究平台。

**关键词** 激光器; 锁模光纤激光器; 声光效应; 光孤子; 光子晶体光纤; 孤子动力学

中图分类号 TN248

文献标志码 A

doi: 10.3788/CJL202148.1901006

### 1 引言

光孤子脉冲是一种常见的超短光脉冲。由于色散与非线性效应的平衡, 光孤子在传播过程中脉冲形状保持不变, 具有一些类似“粒子”的传输特性<sup>[1]</sup>, 使得其在光通信、光频梳、光信号处理、超快激光及非线性光学等领域有重要的研究价值<sup>[2-3]</sup>。同时, 邻近的孤子之间由于相互作用, 可形成各种复杂新奇的束缚孤子态<sup>[4-7]</sup>。对孤子相互作用动力学的研究不仅有助于深刻理解非线性系统内稳态解形成过程的物理机理, 而且在提高通信容量和克服通信系统噪声方面有很大的应用潜力<sup>[8]</sup>。

被动锁模激光器可以实现腔内多脉冲运转和稳

定的谐波锁模, 从而输出超高重复频率的脉冲激光<sup>[9-10]</sup>。同时, 被动锁模激光器也可以用于研究多孤子之间的相互作用, 并在一定程度上实现腔内脉冲孤子调控, 因此被广泛认为是优质的孤子动力学研究平台。2017年, Herink等<sup>[11]</sup>利用色散傅里叶变换技术在钛宝石锁模激光器中观测到了孤子分子的动力学过程。同年, Krupa等<sup>[12]</sup>对锁模光纤激光器中的孤子相互作用进行了理论预测和实验验证。然而, 在传统的被动锁模激光器中, 腔内只有少量的光脉冲, 孤子相互作用过程的样本数少, 并且由于噪声和脉冲间群速度的差异, 很多不可控的孤子碰撞、解离等过程非常容易发生<sup>[13-16]</sup>。最近几年, 研究者在锁模光纤激光器内引入一段实芯光子晶体光纤,

收稿日期: 2021-07-21; 修回日期: 2021-08-19; 录用日期: 2021-09-02

基金项目: 2021年度博士后创新人才支持计划(BX2021328)、张江实验室建设与运行项目(三期)(20DZ2210300)、上海市2021年度“科技创新行动计划”原创探索项目(21ZR1482700)、国家高层次人才青年项目

通信作者: \*pangmeng@siom.ac.cn; \*\*lengyuxin@siom.ac.cn

利用光子晶体光纤纤芯中的 GHz 量级声光效应将激光器谐振腔分割成若干分布均匀、且可钳制光脉冲的势阱,即光机晶格<sup>[17-21]</sup>。当激光器内的脉冲或脉冲结构的重复频率与光子晶体光纤纤芯内声场的谐振频率匹配时,高重复频率脉冲串可通过电致伸缩力驱动此高频谐振声场<sup>[1,19,22]</sup>;而脉冲串驱动的高频谐振声场通过相位调制反作用于激光器内的光脉冲,使其被钳制在谐振声场的每一个周期内,从而形成稳定的光机晶格<sup>[19]</sup>。前期的实验利用光机晶格产生了稳定的 GHz 重复频率超快(亚百飞秒)光纤激光器<sup>[17-18]</sup>,并利用该激光器对激光器腔内大量脉冲孤子进行一定程度上的操控,例如 GHz 脉冲串全光信息的存储<sup>[19]</sup>、孤子超分子态的产生<sup>[20]</sup>、孤子对的可控形成与解离<sup>[21]</sup>。

本文以基于光子晶体光纤中声光效应的锁模光纤激光器为实验平台,观测并研究基于稳定光机晶格的亚稳态激光器工作状态。这种状态在宏观上保持稳定,即光机晶格保持稳定;但在光机晶格的每个势阱内却存在着剧烈且不停歇的多脉冲相互作用。声光锁模光纤激光器的独特性质为研究平行多脉冲复杂相互作用提供了可能性。研究结果表明,对激光器的参数进行调节可实现激光器内孤子脉冲总数和势阱内脉冲数量的调节,从而在一定程度上实现了复杂脉冲间相互作用的调控。

## 2 实验装置

实验所用的声光锁模光纤激光器如图 1 所示,其中 EDF 为掺铒光纤,WDM 为波分复用器,ISO 为隔离器,PCF 为光子晶体光纤, $\Delta\lambda_{\text{FWHM}}$  为光谱带宽。该激光器采用 980 nm 的半导体激光器(LD)作

为泵浦源,双端泵浦 0.6 m 长掺铒光纤放大器。锁模方式为非线性偏振旋转(NPR)锁模,偏振控制器(FPC1)、起偏器(polarizer)及偏振控制器(FPC3)共同产生人工可饱和吸收体效应。系统中置入 1 m 长的光子晶体光纤作为声光锁模元件。第一个 90:10 耦合器(OC1)将腔内 10%的光输出腔外用于检测。50:50 耦合器(OC2)一端连接 45 GHz 带宽光电探测器(PD)和具有 33 GHz 带宽、200-GSa/s 采样率的高速示波器(OSC),用于采集脉冲激光时域信号;另外一端连接耦合器(OC3),OC3 输出一端连接分辨率为 0.02 nm 的光谱仪(OSA)采集光谱信息,OC3 另一端经过 5 km 单模光纤(SMF)进行时域拉伸色散傅里叶变换(TS-DFT)<sup>[6,11,22]</sup>后,接入 PD 和 OSC 端口采集信号。经过 TS-DFT 系统拉伸后的时域脉冲宽度  $\Delta T$  与单模光纤的色散参数  $D$ (在 1550 nm 波长处约为  $18 \text{ ps}\cdot\text{km}^{-1}\cdot\text{nm}^{-1}$ )、脉冲的光谱宽度  $\Delta\omega$ 、单模光纤长度  $L$  成正比。当输入 TS-DFT 系统的脉冲光谱宽度为 1.8 nm 时,如图 1(b)所示,经过时域色散展宽的脉冲宽度  $t_{\text{FWHM}}$  测量值约为 160 ps,如图 1(c)所示,与理论计算值 162 ps 吻合。TS-DFT 系统的实时光谱分辨率由于光电探测器和示波器的带宽限制,约为 0.28 nm。

激光器腔内大部分由普通单模光纤构成,在 1550 nm 波长附近具有较大的负色散值,因此激光器工作在孤子锁模状态。激光器内的高频声光效应器件为一段约 1 m 长的实芯光子晶体光纤[艾菲博(宁波)光电科技有限责任公司]<sup>[19,23-24]</sup>,纤芯直径约为  $1.9 \mu\text{m}$ ,占空比约为 80%,光纤所支持纤芯基模声场的谐振频率为 1.89 GHz。实验中,激光腔腔长约为 21 m,对应激光器的自由光谱范围为 9.8 MHz。

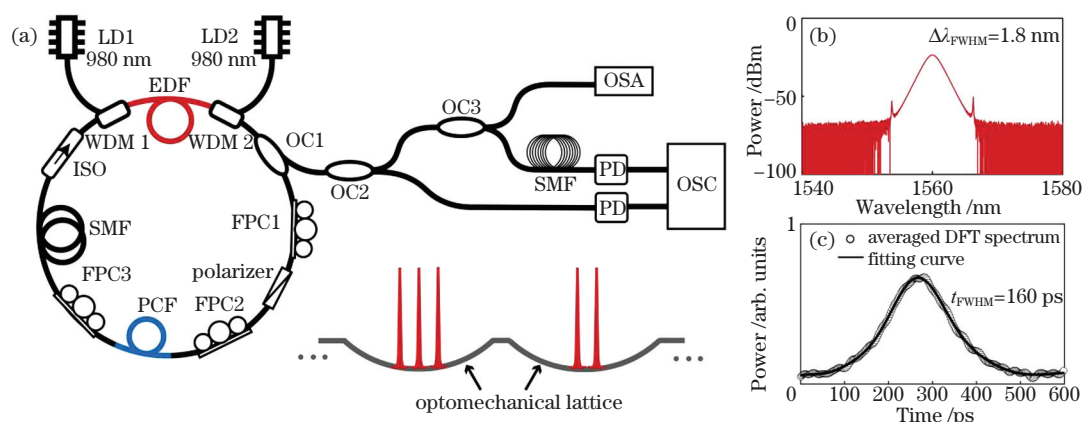


图 1 声光锁模光纤激光器。(a)实验装置图;(b)TS-DFT 输入脉冲光谱图;(c)脉冲经过 5 km 单模光纤展宽后的平均测量时域波形

Fig. 1 Acousto-optic mode-locked fiber laser. (a)Experimental setup; (b) input pulse's spectrum of TS-DFT; (c)average measured time domain waveform of pulse after 5-km single mode fibre stretching

光子晶体光纤内声光效应所产生的光机晶格将激光腔长分为 193 个均匀分布的势阱,激光器脉冲序列重复频率达到 1.89 GHz,对应光子晶体光纤的谐振频率,光机晶格的每一个周期内可束缚一个(或多个)光脉冲。

### 3 实验结果与讨论

在实验中,将双端泵浦半导体激光器的泵浦功率分别调节至约 380 mW,并调节 NPR 锁模元件的工作状态,可实现稳定的谐波锁模。激光器输出光谱图及时域脉冲序列如图 2(a)、(d)所示。从图 2(a)可以看出:输出的脉冲光谱在对数坐标下呈三角形,是双曲线形光谱的典型特征<sup>[25-27]</sup>,且光谱上存在明显的 Kelly 边带<sup>[28-29]</sup>,表明激光器工作在孤子锁模状态下;测量得到的输出光谱中心波长约为 1558 nm,3 dB 带宽为 2.46 nm。从图 2(d)可以看出,在此状态下光机晶格的每个周期内只观测到一个相对简单的脉冲所激发的冲击响应波形。假设光机晶格的每个周期内只钳制一个孤子脉冲,此时脉冲串重复频率为 1.89 GHz,在实验中,通过测量 OC1 输出的激光平均功率,反推出激光腔内的平均功率约为 70 mW,则可计算得到光机晶格单个周期内的脉冲总能量约为 37 pJ。

利用实验测量得到的脉冲光谱宽度,结合孤子脉冲的时间带宽积(0.32)和孤子面积理论,也可以在理论上得到激光器内的单脉冲能量。

$$E_p = -\frac{3.52\beta_2}{\gamma_{\text{Kerr}}\tau_{\text{FWHM}}}, \quad (1)$$

式中: $E_p$  表示单脉冲能量; $\tau_{\text{FWHM}}$  为脉冲时域半峰全宽; $\beta_2$  和  $\gamma_{\text{Kerr}}$  为激光器内的平均色散值与平均非线性系数。实际激光器腔长约为 21 m,其中普通单模光纤长度约为 19.4 m(非线性系数约为  $1.1 \text{ km}^{-1}\cdot\text{W}^{-1}$ ,群速度色散约为  $-22.8 \text{ ps}^2/\text{km}$ ),增益光纤长度约为 0.6 m(非线性系数约为  $9.3 \text{ km}^{-1}\cdot\text{W}^{-1}$ ,群速度色散约为  $77 \text{ ps}^2/\text{km}$ ),实芯光子晶体光纤长度约 1 m(非线性系数约为  $29 \text{ km}^{-1}\cdot\text{W}^{-1}$ ,群速度色散约为  $-120 \text{ ps}^2/\text{km}$ ),故腔内的平均非线性系数为  $2.66 \text{ km}^{-1}\cdot\text{W}^{-1}$ ,平均群速度色散为  $-24.6 \text{ ps}^2/\text{km}$ 。孤子脉冲的 3 dB 光谱宽度为 2.46 nm,时间带宽积为 0.32,可估算出脉冲的  $\tau_{\text{FWHM}}$  约为 1.04 ps。将上述参数代入(1)式,可以得到输出的  $E_p$  约为 32 pJ,与实验中的测量值 37 pJ 符合得较好。因此,在图 2(a)、(d)的工作状态下,光机晶格的每一个周期内只钳制一个孤子光

脉冲。

在实验中,微调 NPR 的工作状态,可改变激光器的工作状态,图 2(b)、(e)和图 2(c)、(f)分别为两次调整后的输出光谱、时域脉冲序列。从图 2(a)~(c)可以看出,在脉冲重复频率(1.89 GHz)保持不变的情况下,输出激光的光谱可发生剧烈变化,脉冲的光谱宽度由 2.46 nm 逐渐降低至 1 nm,甚至 0.6 nm,而在此过程中激光器的输出平均功率基本保持不变,约为 70 mW。从图 2(b)、(c)可以看出,当脉冲光谱变窄到 1 nm 和 0.6 nm 时,未在光谱上观测到明显的 Kelly 边带,是因为当脉冲光谱较窄且未覆盖到 Kelly 边带的相位匹配波长时,无法激发明显的色散波辐射(Kelly 边带)<sup>[20,28-30]</sup>。

在调节 NPR 工作状态的过程中,激光器内的色散与非线性系数不发生改变,可以认为激光器仍然工作在孤子锁模状态下,这可以由在不同状态下观测到的脉冲光谱一直保持三角形(双曲线形光谱)波形得到验证<sup>[25-27]</sup>,如图 2(a)~(c)所示。而对不同状态下脉冲光谱宽度进行测量,即可由脉冲孤子的时间带宽积与孤子面积理论,计算出在不同状态下的单脉冲能量。例如,当脉冲光谱为 1 nm 时,如图 2(b)所示,可估算出脉冲时域半峰全宽约为 2.56 ps,再利用孤子面积理论,可计算出单脉冲能量为 12.7 pJ,再由 70 mW 的激光平均功率和 9.8 MHz 的基频重复频率,可计算得到在此状态下激光腔内同时产生了约 562 个光孤子脉冲,光机晶格每个周期内平均钳制 3 个光脉冲。同理,当脉冲光谱为 0.6 nm 时,如图 2(c)所示,在此状态下激光器的输出平均功率仍为约 70 mW,可估算出脉冲时域半峰全宽约为 4.27 ps,再利用孤子面积理论,可计算出单脉冲能量约为 7.59 pJ,并可计算得到在此状态下激光腔内同时产生了约 941 个光孤子脉冲,光机晶格每个周期内平均钳制 5 个光脉冲。

实验研究表明,当激光器处于图 2(b)、(c)这两个亚稳态的工作状态时,光机晶格可稳定存在,但光机晶格每个周期中钳制住的几个光脉冲会发生复杂的相互作用。从图 2(e)、(f)可以看出,在多脉冲亚稳态工作状态下,每个周期内的时域脉冲波形不同,且在剧烈变化,与图 2(d)的结果完全不同。从图 2(d)稳定的时域波形可以看出,光机晶格每个周期内稳定钳制一个孤子脉冲。而根据图 2(e)、(f)中的时域信号,很难直接读出光机晶格每个周期内钳制几个光脉冲,是由于受到实验中所采用的光电探测器和示波器的带宽限制,测量设备的时域分辨率约为



25 ps, 大于约 10 ps 的孤子脉冲间隔。

不同的激光器工作状态, 稳态如图 2(d) 所示, 亚稳态如图 2(e)、(f) 所示, 可以利用 TS-DFT 技术加以研究, 其中脉冲相互作用现象可利用 TS-DFT 信号予以揭示。在实验中, 激光器输出的光脉冲经过一段 5 km 长的普通单模光纤, 在单模光纤中由

于色散效应, 脉冲在时域上被展宽, 从而得到实时脉冲频谱信息<sup>[11-12]</sup>。当激光器工作在单脉冲的稳定声光锁模状态下时, 如图 2(a)、(d) 所示的状态, TS-DFT 信号如图 3 所示。由图可知, 在此状态下, 光机晶格每一个周期内都稳定钳制住了一个宽谱的孤子脉冲, 且光谱非常稳定。

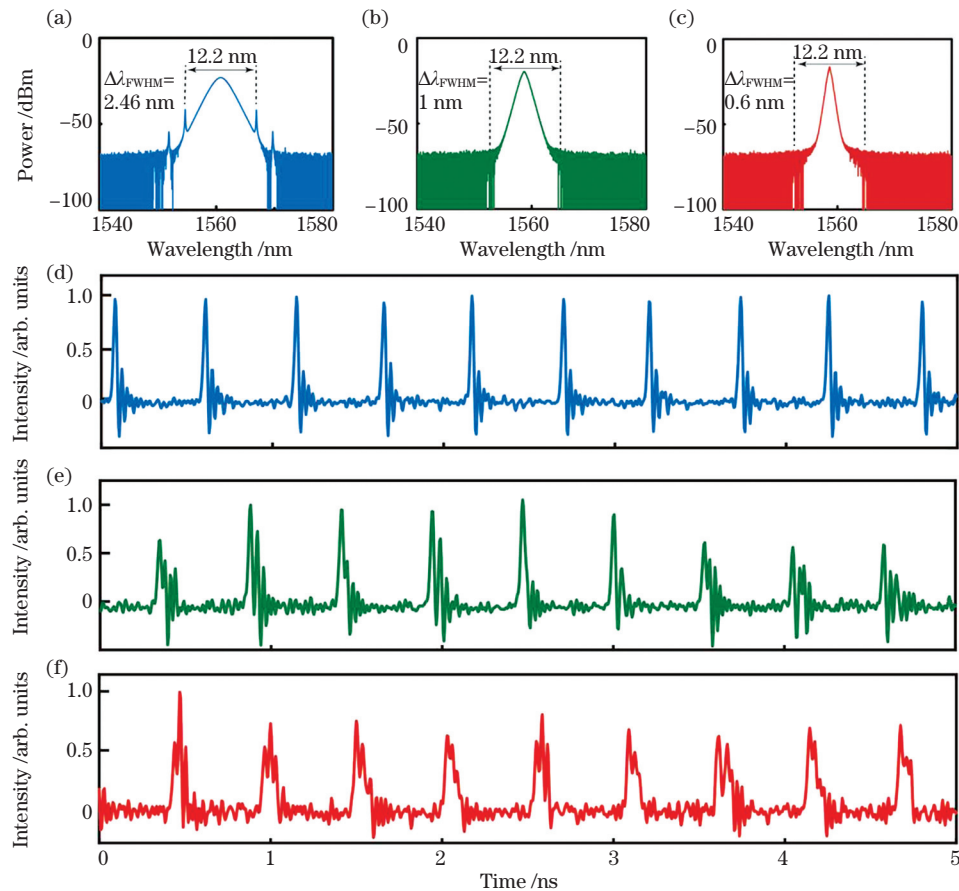


图 2 不同状态下输出光谱及其脉冲时域序列。(a)~(c)输出光谱;(d)~(f)脉冲时域序列  
Fig. 2 Output spectra and their pulse time-domain sequences under different states. (a)~(c) Output spectra;  
(d)~(f) pulse time-domain sequences

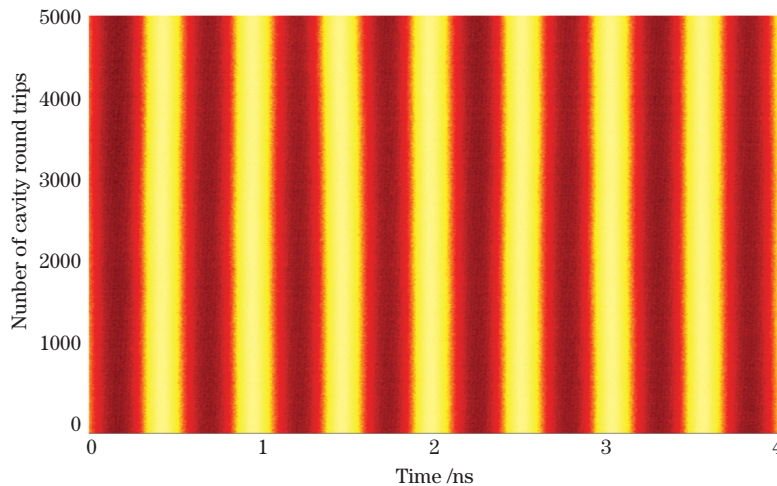


图 3 光机晶格每个周期内仅束缚一个脉冲时的 DFT 图  
Fig. 3 DFT diagram when only one soliton trapped in each cycle of optomechanical lattice

当光机晶格的一个周期内存在多个光脉冲时,相互靠近的孤子经过色散光纤展宽后在时域上重叠,会发生光谱干涉,干涉条纹的疏密反映了孤子之间的时域间隔,干涉条纹相对于包络的移动对应孤子间相对相位的变化<sup>[11-12]</sup>。因此 TS-DFT 信号的干涉谱演化可直接反应脉冲之间的相位差和时域间隔的变化。当激光器在图 2(b)、(e)的亚稳态工作状态时,输出的时域脉冲演化和 TS-DFT 信号演化如图 4(a)、(b)所示。从图 4(b)可以看出,在此亚稳态下,光机晶格每个周期内都束缚了不止一个光孤子,并且孤子间的相位差和距离都在发生剧烈的变化,说明脉冲孤子之间正在发生复杂的相互作用。但值得一提的是,由于声光效应,激光器内产生了一个稳定的光机晶格,光机晶格的每一个周期内都存在一个强有力的势阱<sup>[19-20]</sup>,即使势阱内发生了剧烈且复杂的孤子间相互作用,仍不能破坏光机晶格,即激光器内的脉冲光场和光子晶体光纤内的 GHz 声场一直保持耦合锁定状态。

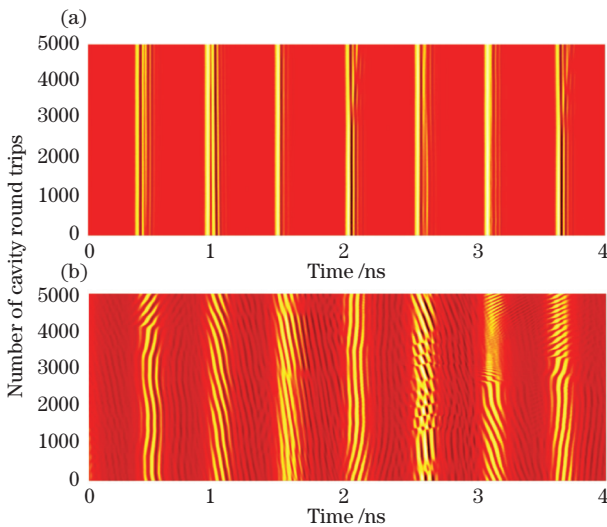


图 4 激光器工作在约 3 个光孤子被束缚在光机晶格每一个周期内的亚稳态状态时的时域与 DFT 信号。

(a)时域信号;(b) DFT 信号

Fig. 4 Time-domain signal and DFT signal of laser working in the metastable state in which about 3 optical solitons trapped in each cycle of optical mechanical lattice. (a) Time-domain signal;

(b) DFT signal

当激光器工作在图 2(c)、(f)的亚稳态工作状态时,时域脉冲演化和 TS-DFT 信号演化如图 5 所示。从图中可以看出,随着脉冲数量的增加,脉冲间的相互作用更为复杂。但在此状态下,光机晶格仍然保持稳定,在每个周期内持续发生更为复杂、激烈

的脉冲间相互作用。实验成功测量了激光器亚稳态工作状态下的复杂 TS-DFT 信号,反应了此状态下光机晶格周期内的多孤子复杂相互作用情况。下一阶段,可利用此平台研究复杂的多脉冲相互作用过程和机理,但需要进一步研发先进的多脉冲 TS-DFT 信号解调算法<sup>[6]</sup>,并利用该算法根据复杂的 TS-DFT 信号反演出多脉冲( $n > 4$ )情况下的脉冲间隔和脉冲相位演化。

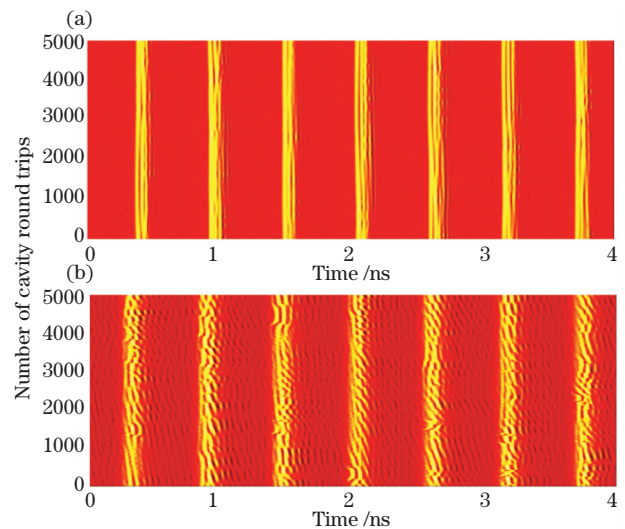


图 5 激光器工作在约 5 个光孤子被束缚在光机晶格每一个周期内的亚稳态状态时的时域与 DFT 信号。

(a)时域信号;(b) DFT 信号

Fig. 5 Time-domain signal and DFT signal of laser working in the metastable state in which about 5 optical solitons trapped in each cycle of optical mechanical lattice. (a) Time-domain signal;

(b) DFT signal

需要指出的是,实验中可以在一定程度上连续调节 NPR,从而连续调节激光器内存在的脉冲数和脉冲的光谱宽度。在调节过程中,光机晶格保持稳定,且激光器的平均输出功率基本保持不变,激光器一直工作在可连续调谐的亚稳态工作状态。虽然上述实验结果只展示了两组亚稳态结果(光机晶格每个周期内平均钳制 3 个和 5 个孤子脉冲),但在相近的平均功率下,本实验组观测到了一系列亚稳态的工作状态。在这些状态下,光机晶格每个周期内的平均脉冲数从约 0.5 个到超过 6 个,对应激光器腔内同时存在从约 100 个到超过 1000 个孤子脉冲。这些现象产生的原因可能为:调节 NPR 工作状态,可以调节激光器内损耗随脉冲峰值功率的变化曲线;在保持低激光峰值功率对应高腔损耗(等效可饱和吸收效应)的同时,调节 NPR 的工作点,可调节

激光峰值功率较高情况下激光器的损耗值,从而调节激光器内所支持的最高脉冲峰值功率;在激光器平均功率一定的情况下,激光器腔内存在的孤子脉冲总数就会改变;在光机晶格不被破坏的情况下,每个周期内所钳制的光脉冲个数就会发生相应的改变。当多个脉冲被钳制在同一个光机晶格周期内时,脉冲间即会发生剧烈且复杂的相互作用。因此,高频声光效应下锁模激光器内具有多脉冲亚稳态工作状态,拥有一定的可调谐能力,可为研究锁模激光器内大量脉冲的相互作用过程与机理提供一个理想的研究平台。

## 4 结 论

报道了基于光子晶体光纤声光效应的高频锁模光纤激光器中存在众多可调控的亚稳态工作状态。改变激光器内 NPR 的工作点,可以在一定程度上实现势阱内脉冲数量和单脉冲能量的调节,而在此调节下声光效应所产生的光机晶格仍然可保持优秀的稳定性。基于效应的锁模光纤激光器中的每一个光机晶格周期内都可以良好地束缚多个发生复杂相互作用的孤子脉冲,使该激光器有潜力成为理想的多孤子动力学研究平台。

## 参 考 文 献

- [1] Agrawal G P. Nonlinear fiber optics [M]. 3rd ed. San Diego: Academic Press, 2001.
- [2] Stegeman G I, Segev M. Optical spatial solitons and their interactions: universality and diversity [J]. Science, 1999, 286(5444): 1518-1523.
- [3] Grellu P, Akhmediev N. Dissipative solitons for mode-locked lasers [J]. Nature Photonics, 2012, 6(2): 84-92.
- [4] Zavyalov A, Iliev R, Egorov O, et al. Discrete family of dissipative soliton pairs in mode-locked fiber lasers [J]. Physical Review A, 2009, 79(5): 053841.
- [5] Zavyalov A, Iliev R, Egorov O, et al. Dissipative soliton molecules with independently evolving or flipping phases in mode-locked fiber lasers [J]. Physical Review A, 2009, 80(4): 043829.
- [6] Wang Z Q, Nithyanandan K, Coillet A, et al. Optical soliton molecular complexes in a passively mode-locked fibre laser [J]. Nature Communications, 2019, 10(1): 830.
- [7] Grapinet M, Grellu P. Vibrating soliton pairs in a mode-locked laser cavity [J]. Optics Letters, 2006, 31(14): 2115-2117.
- [8] Haus H A, Wong W S. Solitons in optical communications [J]. Reviews of Modern Physics, 1996, 68(2): 423-444.
- [9] Amrani F, Haboucha A, Salhi M, et al. Passively mode-locked erbium-doped double-clad fiber laser operating at the 322nd harmonic [J]. Optics Letters, 2009, 34(14): 2120-2122.
- [10] Zhao L M, Tang D Y, Liu D. Ultrahigh-repetition-rate bound-soliton fiber laser [J]. Applied Physics B, 2010, 99(3): 441-447.
- [11] Herink G, Kurtz F, Jalali B, et al. Real-time spectral interferometry probes the internal dynamics of femtosecond soliton molecules [J]. Science, 2017, 356(6333): 50-54.
- [12] Krupa K, Nithyanandan K, Andral U, et al. Real-time observation of internal motion within ultrafast dissipative optical soliton molecules [J]. Physical Review Letters, 2017, 118(24): 243901.
- [13] Jang J K, Erkintalo M, Murdoch S G, et al. Ultraweak long-range interactions of solitons observed over astronomical distances [J]. Nature Photonics, 2013, 7(8): 657-663.
- [14] Kodama Y, Wabnitz S, Romagnoli M. Soliton stability and interactions in fibre lasers [J]. Electronics Letters, 1992, 28(21): 1981-1983.
- [15] Roy V, Olivier M, Babin F, et al. Dynamics of periodic pulse collisions in a strongly dissipative-dispersive system [J]. Physical Review Letters, 2005, 94(20): 203903.
- [16] Weng W L, Bouchand R, Lucas E, et al. Polychromatic Cherenkov radiation induced group velocity symmetry breaking in counterpropagating dissipative Kerr solitons [J]. Physical Review Letters, 2019, 123(25): 253902.
- [17] Pang M, Jiang X, He W, et al. Stable subpicosecond soliton fiber laser passively mode-locked by gigahertz acoustic resonance in photonic crystal fiber core [J]. Optica, 2015, 2(4): 339-342.
- [18] He W, Pang M, Menyuk C R, et al. Sub-100-fs 1.87 GHz mode-locked fiber laser using stretched-soliton effects [J]. Optica, 2016, 3(12): 1366.
- [19] Pang M, He W, Jiang X, et al. All-optical bit storage in a fibre laser by optomechanically bound states of solitons [J]. Nature Photonics, 2016, 10(7): 454-458.
- [20] He W, Pang M, Yeh D H, et al. Formation of optical supramolecular structures in a fibre laser by tailoring long-range soliton interactions [J]. Nature Communications, 2019, 10: 5756.
- [21] He W, Pang M, Yeh D H, et al. Synthesis and dissociation of soliton molecules in parallel optical-soliton reactors [J]. Light, Science & Applications, 2021, 10: 1901006-6.

- 2021, 10(1): 120.
- [22] Kang M S, Nazarkin A, Brenn A, et al. Tightly trapped acoustic phonons in photonic crystal fibres as highly nonlinear artificial Raman oscillators [J]. *Nature Physics*, 2009, 5(4): 276-280.
- [23] Goda K, Jalali B. Dispersive Fourier transformation for fast continuous single-shot measurements [J]. *Nature Photonics*, 2013, 7(2): 102-112.
- [24] ifiber[EB/OL]. [2021-07-15]. <http://www.ifiber-global.com>.
- [25] Sala K L, Kenney-Wallace G A, Hall G E. CW autocorrelation measurements of picosecond laser pulses [J]. *IEEE Journal of Quantum Electronics*, 1980, 16(9): 990-996.
- [26] Kim J, Song Y J. Ultralow-noise mode-locked fiber lasers and frequency combs: principles, status, and applications[J]. *Advances in Optics and Photonics*, 2016, 8(3): 465-540.
- [27] Song Y, Jung K, Kim J. Impact of pulse dynamics on timing jitter in mode-locked fiber lasers [J]. *Optics Letters*, 2011, 36(10): 1761-1763.
- [28] Kelly S M J. Characteristic sideband instability of periodically amplified average soliton[J]. *Electronics Letters*, 1992, 28(8): 806-807.
- [29] Gordon J P. Dispersive perturbations of solitons of the nonlinear Schrödinger equation[J]. *Journal of the Optical Society of America B*, 1992, 9(1): 91-97.
- [30] Wang Y T, Fu S N, Zhang C, et al. Soliton distillation of pulses from a fiber laser[J]. *Journal of Lightwave Technology*, 2021, 39(8): 2542-2546.

## Complex Multi-Pulse Interactions in Harmonic Mode-Locked Fiber Laser Based on Acousto-Optic Effect

Zhang Xintong<sup>1,2</sup>, Wang Xiaocong<sup>1,2</sup>, Huang Qi<sup>3</sup>, Huang Zhiyuan<sup>2</sup>, Luo Zhuozhao<sup>5</sup>,  
Zhou Gengji<sup>2</sup>, Jiang Xin<sup>4,5</sup>, Leng Yuxin<sup>2,3\*</sup>, Pang Meng<sup>1,2,3\*</sup>

<sup>1</sup>Department of Optics and Optical Engineering, University of Science and Technology of China, Hefei, Anhui 230026, China;

<sup>2</sup>State Key Laboratory of High Field Laser Physics, Shanghai Institute of Optics and Fine Mechanics, Chinese Academy of Sciences, Shanghai 201800, China;

<sup>3</sup>School of Physics and Optoelectronic Engineering, Hangzhou Institute for Advanced Study, University of Chinese Academy of Sciences, Hangzhou, Zhejiang 310013, China;

<sup>4</sup>Russell Division, Max Planck Institute for the Science of Light, Erlangen, 91058, Germany;

<sup>5</sup>National Engineering Laboratory for Fiber Optic Sensing Technology, Wuhan University of Technology, Wuhan, Hubei 430070 China

### Abstract

**Objective** Because of their high application potential in long-distance optical communications and ultrafast laser physics, optical solitons, which are localized structures in nonlinear systems, have piqued the interest of researchers. During long-distance propagation, optical solitons can interact with each other, resulting in a variety of bound-soliton states known as “soliton molecules”. Therefore, mode-locked lasers that can support the long-distance propagation of multiple solitons within their cavities are widely regarded as ideal platforms for studying soliton interactions and dynamics. However, the studies of the complex interactions of several optical solitons are difficult in traditional passive mode-locked lasers because fast drifts and the frequent collisions of solitons caused due to intense soliton interactions can degrade the stability of the laser mode-locking operation. In this paper, we use a high-repetition-rate optomechanically mode-locked fiber laser to successfully study the complex interactions of many optical solitons. The strong optomechanical effect in a short length of solid-core photonic crystal fiber (PCF) allows forming a robust optomechanical lattice in the laser cavity, and multiple solitons can be stably trapped within each cycle of the optomechanical lattice. Experimental results reveal that complex soliton interactions can be observed and partially controlled in this optomechanically mode-locked fiber laser, highlighting the significant potential of this unique optomechanical fiber laser system for studying complex soliton dynamics.

**Methods** To investigate the complex phenomena of multi-pulse interactions, we created an optomechanically mode-locked fiber laser with a short solid-core PCF length as the harmonically mode-locking element. Because of the strong coupling between optical and acoustic waves in the PCF, a robust optomechanical lattice formed in the laser cavity,



dividing the laser cavity into two halves. Multiple solitonic pulses can be trapped within each of these time-slots, working as an optical-soliton “reactor.” The stability of the optomechanical lattice is largely enhanced by the strong optomechanical interactions in the PCF core. In contrast, the multiple solitons trapped in each lattice cycle were observed to interact intensely with each other.

In the experiments (Fig. 1), an erbium-doped fiber amplifier was used with two 980 nm laser diodes as the pump sources. Two polarization controllers working together with an optical polarizer acted as an artificial saturable absorber through nonlinear polarization rotation (NPR). A time-stretch dispersion Fourier transform (TS-DFT) setup was built using a 5-km-long single-mode fiber (SMF) as the stretching element to demonstrate the detailed information of the multi-soliton interaction processes. Two 45-GHz bandwidth detectors and a 33-GHz bandwidth oscilloscope were used to record the laser output pulses' time-domain trace and DFT signal. Furthermore, the laser output spectrum was recorded using an optical spectrum analyzer with a resolution of 0.02 nm. Since most of the laser cavity was made from SMF, the cavity dispersion was strongly anomalous with a calculated average value of  $-23.8 \text{ ps}^2/\text{km}$ , leading to soliton operation of the laser with hyperbolic pulse shape.

**Results and Discussions** By carefully adjusting the intra-cavity polarizer controllers, stable harmonic mode-locking at 1.89 GHz resonance frequency of the acoustic core resonance in the PCF could be realized when both of the two pump diodes have pump powers of approximately 380 mW at 980 nm. The laser output spectrum, as well as the time-domain pulse sequence, were captured. When only one soliton is trapped in each cycle of the optomechanical lattice, the stable acousto-optic mode-locking state could be obtained with a 3 dB spectral bandwidth of 2.46 nm [Fig. 2(a) and Fig. 2(d)]. At this state, a strong Kelly-sideband observed on the pulse spectrum indicates that the laser was operating in the soliton regime. Through the experiments, we found that by adjusting the intra-cavity polarizer controllers, the laser output spectrum could be varied gradually from 2.46 nm to less than 0.6 nm [Figs. 2(b)–(f)], while the optomechanical lattice remained to be stable and the average output power of the laser was kept almost constantly at approximately 70 mW, giving rise to a series of quasi-stable acousto-optic mode-locking states. In those states, multiple soliton pulses were trapped within each cycle of the optomechanical lattice. The DFT signal unveiled that intense and complex interactions between the trapped solitons occurred within each cycle of the lattice (Figs. 3–5). As an entire, this optomechanically mode-locked fiber laser system permits several solitons to coexist in its cavity, and complex interactions between these solitons in one cycle could be studied in the future using this unique platform.

**Conclusions** In the experiments, we obtained a large number of quasi-stable states in an optomechanically mode-locked fiber laser. We discovered that each isolated cycle of the optomechanical lattice could function as robust optical-soliton “reactors,” allowing us to study complex and intense soliton interactions. We could partially adjust the number of pulses trapped in each cycle of the optomechanical lattice and, thus, the total number of solitons generated in the laser cavity by adjusting the working point of the NPR effect in the laser cavity. In this way, we could control to some extent the multi-soliton interaction processes. Compared with a traditional passive mode-locked laser, this system's stability, flexibility, and high-repetition-rate features make it an ideal experimental platform for studying complex multi-soliton interactions, providing some useful insights on soliton dynamics.

**Key words** lasers; mode-locked fibre laser; acousto-optic effect; soliton; photonic crystal fiber; soliton dynamics

**OCIS codes** 140.3538; 140.3538; 140.4050